CHEMISTRY
A EUROPEAN JOURNAL

DOI: 10.1002/chem.200700618

Shape- and Phase-Controlled Synthesis of Monodisperse, Single-Crystalline Ternary Chalcogenide Colloids through a Convenient Solution Synthesis Strategy

Weimin Du, Xuefeng Qian,* Jie Yin, and Qiang Gong[a]

Abstract: Colloidal, monodisperse, single-crystalline pyramidal $CuInS_2$ and rectangular $AgInS_2$ nanocrystals were successfully synthesized through a convenient and improved solvothermal process that uses hexadecylamine as a capping reagent. The crystal phase, morphology, crystal lattice, and chemical composition of the as-prepared products were characterized by using X-ray diffraction, transmission electron microscopy (TEM), high-resolution TEM, and energy dispersive X-ray spectroscopy. Results revealed that the as-synthesized $CuInS_2$ colloid is in the tetragonal phase (size: 13–17 nm) and the $AgInS_2$ in the orthorhombic structure (size: 17 ± 0.5 nm). A possible shape evolution and crystal growth mechanism has been suggested for the formation of pyramidal $CuInS_2$ and rectangular $AgInS_2$ colloids. Control experiments indicated that the morphology- and/or phase-change of $CuInS_2$ and orthorhombic $AgInS_2$ colloids are temperature- and/or time-dependent. $CuInS_2$ colloids absorb well in the range of visible light at room-temperature, indicating its potential application as a solar absorber. Two photoluminescence (PL) subbands at 1.938 and 2.384 eV in the PL spectra of $CuInS_2$ colloids revealed that the recombination of the closest and the second closest donor–acceptor pairs within the $CuInS_2$ lattice, in which the donor defect (Cu_i) occupies an interstitial position and the acceptor defect (V_{In}) resides at an adjacent cation site. In addition, the synthesis strategy developed in this study is convenient and inexpensive, and could also be used as a general process for the synthesis of other pure or doped ternary chalcogenides that require a controlled size (or shape). This process could be extended to the synthesis of other functional nanomaterials.

Keywords: colloids · crystal growth · functional materials · monodisperse · ternary chalcogenides

Introduction

Ternary chalcogenides of I-III-VI (I = Cu, Ag; III = Ga, In; VI = S, Se, Te) have attracted considerable attention owing to their excellent electrical and optical properties, and their important technological applications in areas such as photovoltaic solar cells, linear and nonlinear optical instruments, and light emitting diodes.[1] As one of the most important ternary chalcogenides, $CuInS_2$ is in development as a light absorber for harvesting solar energy, owing to its high absorption coefficient ($\alpha\approx5\times10^5\ cm^{-1}$) and optimal band gap energy (1.45 eV), which is close to solar energy (1.1–1.5 eV), low-cost production, and low toxicity.[2] To date, solar cells based on $CuInS_2$-derived photovoltaic materials have achieved 12–13% conversion efficiencies on large area modules,[2a] and efficiencies close to 18% have been achieved under laboratory conditions.[2e] It has been reported in the literature that the high conversion efficiency of ternary chalcogenides is generally caused by the hole-energy barrier at grain boundaries, thus preventing the electron-hole recombination process or the formation of random p–n junctions throughout the inhomogeneous polycrystalline thin film.[3] Additionally, $AgInS_2$ has an orthorhombic (*o*-) structure or chalcopyrite-like (*c*-) structure, and is an intriguing functional material, owing to its promising applications in photovoltaic and optoelectronic fields.[4] Thus, the preparation of monodisperse single-crystalline colloids of compounds I-III-VI might improve their photovoltaic performances, because a larger amount of "grain boundaries" and p-n junctions can be formed. However, only solid thin films, or irregular particles that have ill-controlled size/morphologies, have been obtained in the past few years, through processes such as

[a] Dr. W. Du, Prof. X. Qian, Prof. J. Yin, Dr. Q. Gong
School of Chemistry and Chemical Technology
Shanghai Jiao Tong University, Shanghai 200240 (China)
Fax: (+86) 21-5474-1297
E-mail: xfqian@sjtu.edu.cn

Supporting information for this article is available on the WWW under http://www.chemeurj.org/ or from the author.

the elemental hydrothermal or solvothermal technique,[5] the single-source precursor route[6] or high-temperature epitaxial growth.[7] More recently, some progress has been made on the controlled synthesis of the ternary chalcogenides, for example, $ZnIn_2S_4$ nanotubes or nanoribbons have been prepared by a pyridine solvothermal method, $AgInSe_2$ nanorods have been formed by means of the single-source precursor route, and $CuInSe_2$ nanowires through the Au-catalyzed vapor–liquid–solid growth process.[8] Therefore, the challenge remains, how to prepare monodisperse ternary chalcogenide colloids that have controlled size and shape through a facile, inexpensive, and general method. The obtained colloids might provide a straightforward route by using the spin coating process for the production of solar cell devices.

Nevertheless, precise control of the chemical composition, crystal structure, size, shape, and surface chemistry of nanomaterials allows one to observe their unique properties, and to be able to tune their chemical and physical properties as desired.[9] In the past decade, great progress has been made in the controlled synthesis of colloidal monodisperse binary chalcogenides and other functional compounds, through the organic solution-phase pyrolysis approach.[10] Compared with the significant progress in monodisperse binary chalcogenide colloids, research on ternary chalcogenide colloids has been limited, owing to the lack of suitable synthetic methods.

In this study, a convenient and general synthesis strategy was developed to prepare monodisperse $CuInS_2$ and $AgInS_2$ colloids through a modified-surfactant solvothermal approach. Typical samples were prepared by an improved-solvothermal process with hexadecylamine (HDA) as the capping reagent. The processes were carried out in anisole with some simple precursors, for example, metal acetate, chloride, or nitrate and carbon disulfide. The obtained products could be readily redispersed in organic solvents (e.g., toluene and chloroform) and self-assembled into colloidal monolayers over a large area. Experimental conditions and results are summarized in Table 1 and in the Supporting Information, Table S1.

Table 1. Experimental parameters and results of $CuInS_2$.[a]

TEM Figure no.	Capping reagents[b]	T [°C]	t [h]	Morphologies
2a,c,e, 7d	HDA	200	12	monodisperse colloids
4a	HDA	200	2	agglomeration
4b	HDA	200	6	aggregated particles
4c	HDA	200	24	monodisperse colloids
7a	HDA	120	12	agglomeration
7b	HDA	160	12	monodisperse colloids
7c	HDA	180	12	monodisperse colloids
S2a	ODA	200	12	monodisperse colloids
S2b	DDA	200	12	aggregated particles

[a] For a typical experiment see the Experimental Section; [b] HDA: hexadecylamine, ODA: octadecylamine, DDA: dodecylamine; [c] The crystal phase of the $CuInS_2$ synthesized in present work was kept unchanged.

Results and Discussion

Crystal phase, compositional, morphological, structural characterization and shape evolutional analysis of typical $CuInS_2$ and $AgInS_2$ colloids: The crystal phase of the as-synthesized products was identified by powder X-ray diffraction (XRD) and energy dispersive X-ray spectroscopy (EDS) (Figure 1).

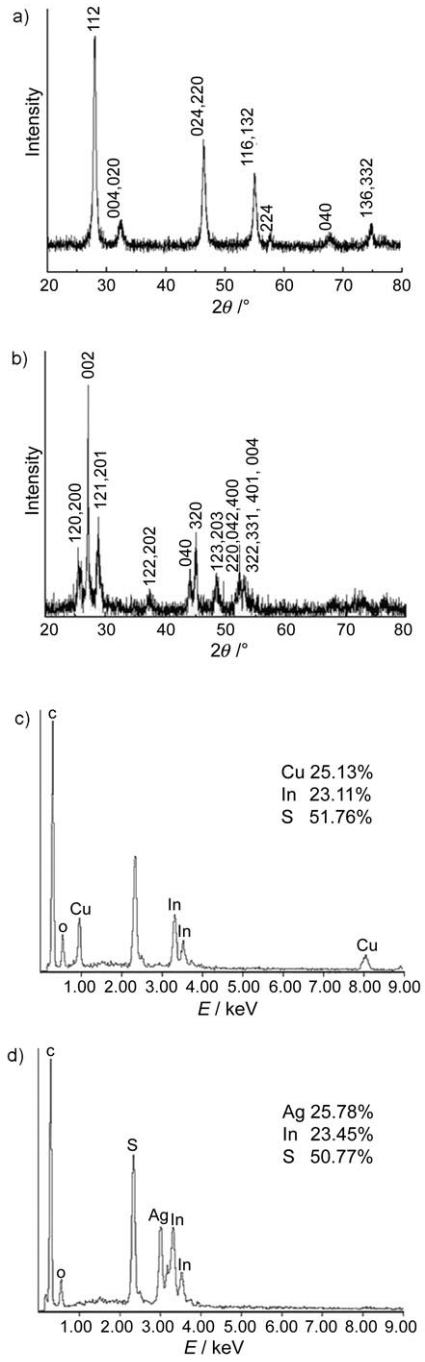

Figure 1. XRD patterns and EDS spectra of $CuInS_2$ (a,c) and $AgInS_2$ (b,d), respectively. The carbon signal in the EDS spectra is from trace HDA capped onto as-synthesized colloids and the oxygen signal might come from air or slight oxidization of the product.

The XRD pattern shown in Figure 1a clearly reveals that all of the diffraction peaks match well with the tetragonal $CuInS_2$ (lattice parameters: $a=5.52$ and $c=11.12$ Å, JCPDS 47–1372; *I*-42*D*). Under similar reaction conditions, orthorhombic $AgInS_2$ (lattice parameters: $a=7.001$, $b=8.278$, and $c=6.698$ Å, JCPDS 25–1328; *Pna*21) could also be prepared in its metastable phase (Figure 1b). It is well known that the orthorhombic phase of $AgInS_2$ is usually stable at high temperature (>620 °C), while the tetragonal phase is stable below 620 °C.[4c,6a] The synthesis of the metastable orthorhombic $AgInS_2$, obtained at lower temperatures in our present work, could be ascribed to the change of the chemical growth environment, and the usage of solvent and/or surfactants that result in a temporary phase reversion.[6a] Similar crystal phase reversion phenomena have also appeared in the case of hexagonal wurtzite ZnS and ε-Co colloids.[11] EDS analysis showed that the atom content ratio of Cu, In and S in $CuInS_2$ is 1:0.92:2.06, this in good agreement with the $CuInS_2$ defect structure (namely, the donor defect Cu_i and the acceptor defect V_{In}) (Figure 1c). The atom content ratio of 1:0.91:1.97 for Ag, In, and S in *o*-$AgInS_2$ also corresponds with its defect structure (Ag_i and V_{In}) (Figure 1d).

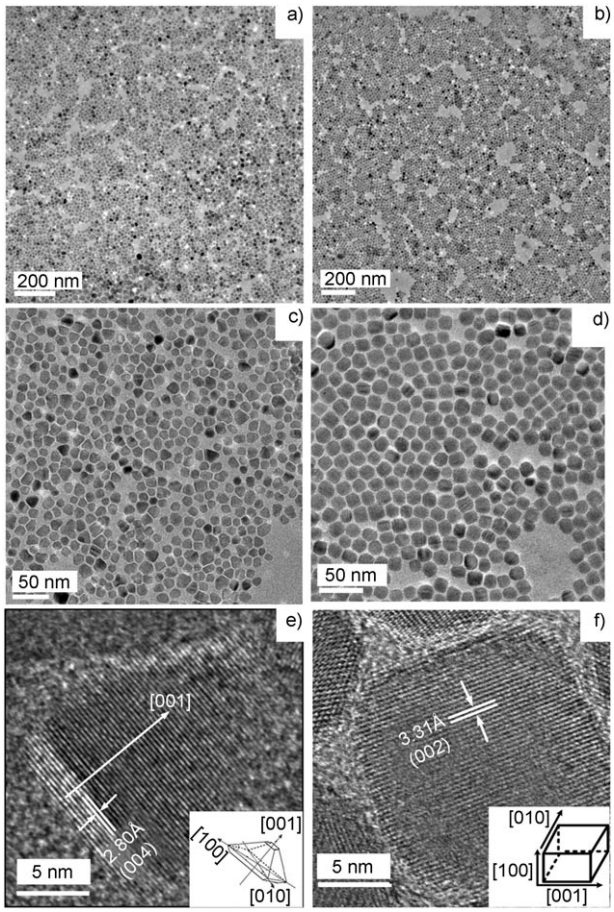

Figure 2. Representative TEM images of $CuInS_2$ (a,c) and $AgInS_2$ (b,d), respectively. HR-TEM images of the $CuInS_2$ (e) and *o*-$AgInS_2$ (f) colloids, respectively (the insert pictures are the corresponding structural sketch maps).

Transmission electron microscopy (TEM) and high-resolution TEM (HR-TEM) evidenced the shape and the corresponding crystallographic orientation of the as-synthesized colloids (Figure 2). Representative TEM images (Figure 2a,b) showed that monodisperse $CuInS_2$ and *o*-$AgInS_2$ colloids were the exclusive products and they can be self-assembled into a colloidal monolayer over a large area. Larger magnification TEM images of $CuInS_2$ and *o*-$AgInS_2$ colloids (Figure 2c,d) showed that the colloidal $CuInS_2$ nanocrystals were polyhedral (sizes: 13–17 nm) and the *o*-$AgInS_2$ colloids were rectangular (size: 17 ± 0.5 nm). Clear lattice fringes in the HR-TEM images (Figure 2e,f) indicate that the as-obtained ternary chalcogenide colloids have a single-crystalline structure. The 2.80 Å lattice space shown in Figure 2e is consistent with the {004} faces *d* spacing of tetragonal $CuInS_2$, this indicates a fast growth along the $<001>$ direction. The lattice fringes in Figure 2f are separated by 3.31 Å, these correspond to the {002} planes of *o*-$AgInS_2$. These results indicate that monodisperse single-crystalline $CuInS_2$ and *o*-$AgInS_2$ colloids can be prepared on a large scale, through the present modified-surfactant solvothermal method.

Generally, the final shape of nanocrystals is dominated by the inherent crystal structure during the initial nucleation stage, and the subsequent growth stage through the delicate control of external factors, for example, surfactants, temperature, and time.[12] In the present system, we think that the crystal shapes of the $CuInS_2$ and *o*-$AgInS_2$ colloids are determined mainly by their inherent crystal structure. The surfactant HDA fulfills the capping reagent role, i.e., capping on the colloid surface, to provide steric hindrance and to prevent the colloids from aggregating. The Gibbs–Curie–Wulff's theorem is represented in Equation (1), in which γ_n is the surface tension of crystal face *n*, and h_n is the distance of that face from the Wulff's point in the crystal.

$$\frac{\gamma_1}{h_2}=\frac{\gamma_2}{h_2}=\frac{\gamma_3}{h_3}=\cdots=\text{constant} \quad (1)$$

Higher surface tension faces tend to grow along the normal direction and eventually disappear from the final appearance.[13a] According to the Donay–Harker rules,[13b] the surface energy of the {001} faces in tetragonal $CuInS_2$ is $\approx$1.4 times larger than that for the {101} faces. Based on the crystal parameters of $CuInS_2$, a sequence of $\gamma_{\{100\}}=\gamma_{\{010\}}\leqslant\gamma_{\{001\}}$ can be deduced from the distances between these three faces and the Wulff's point, which leads to a faster crystal growth along the $<001>$ direction. Furthermore, from the viewpoint of crystal structure, the (001) facets in $CuInS_2$ are terminated by metal ions (Cu^{2+} and In^{3+}), and the (00−1) facets by S^{2-}, these are similar to those of hexagonal ZnO (Figure 3).[13c] On the other hand, the species of M-$(S_2CNHR)_n$ (e.g., $M=In^{3+}$) and $C_{16}H_{33}NH_3^+$ might also be formed within the present synthesis system if the following reaction occurs [Eq. (2)];[13d]

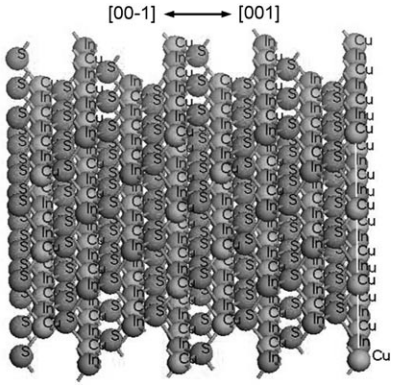

Figure 3. The structural side elevation images of $CuInS_2$ perpendicular to the $\pm$[001] direction. The spatial coordinates of different atoms in $CuInS_2$ are Cu (0 0 0), In (0 0 0.5) and S (0.2295 0.25 0.125), (S. C. Abrahams, J. L. Bernstein, *J. Chem. Phys.* **1973**, *59*, 5415).

$$M^{n+} + 2nC_{16}H_{33}NH_2 + nCS_2 \rightarrow M(S_2CNHC_{16}H_{33})_n + nC_{16}H_{33}NH_3^+ \quad (2)$$

Simultaneously, the newly-formed H_2S, that results from the reaction of CS_2 and hydrated water, could combine with $C_{16}H_{33}NH_2$ to yield the $C_{16}H_{33}NH_3^+$ and S^{2-} species. Through Coulombic interactions, these cations ($C_{16}H_{33}NH_3^+$) would preferentially adsorb onto the negative polar surface of the (00−1) facets and provide a larger steric hindrance. Therefore, $CuInS_2$ colloids would preferentially grow along the $+c$-axis and would be retarded in the $-c$-axis direction (as illustrated in the insert of Figure 2e). As a result, a truncated pyramidal $CuInS_2$ was formed, owing to the incomplete evolution of higher energy (001) surfaces. This phenomenon of the retarded growth in the $-c$-axis direction has also appeared in ZnO nanorods.[14a] The multiangular shapes shown in the TEM images may be a result of the different facets of the truncated pyramids sitting on the copper mesh. This has also been observed for hexagonal pyramidal CoO,[14b] ZnO,[14c] and bullet-shaped tetragonal TiO_2[14d] nanocrystals. For the *o*-$AgInS_2$ obtained here, the surface tension values of {100}, {010}, and {001} are very similar, a result of the closer distance between these three faces and the Wulff's point, this results in a more average growth rate along their directions. As a result, rectangular or quasi-cubic *o*-$AgInS_2$ colloids were formed.

Organic-ligand molecules (e.g., alkyl amines, fatty acids, alkyl thiols, alkyl phosphine oxides, or some nitrogen-containing aromatics) are often used as organic solvents or capping reagents in various processes to prepare monodisperse colloids, including, organic solution-phase pyrolysis[10a] the LSS (liquid-solid-solution) process, microwave-assisted methodology, and solvent-less decomposition of metal thiolate single source precursors. [15] These organic-ligand molecules contain both metal coordinating groups and solvophilic groups, which could dynamically solvate nanocrystals and further control the size and/or morphology of the final products. In the present work, alkyl amines (e.g., HDA) were successfully introduced into the solvothermal process, and they played an important role in forming monodisperse $CuInS_2$ or *o*-$AgInS_2$ colloids. Alkyl amines solubilize the precursors in organic solvents by coordinating with the metal precursors through electron-donating groups. The minimum amount of alkyl amine to be used was determined by the coordination number between metal ions and alkyl amines. Second, they cap the freshly formed nuclei and further moderate the surface of nanocrystals.

In a traditional organic solution-phase pyrolysis system, highly monodisperse colloids are formed in one-step, because a large amount of capping reagent molecules (sometimes used as high temperature solvents) rapidly cap the surface of the nuclei and to prevent further growth and aggregation. However, our results show that as the reaction progresses the formation of highly monodisperse $CuInS_2$ colloids involves three steps, conglomeration, gradual dispersion, and then monodispersion to form the colloids (Figure 4a–c). This is likely a result of the use of less HDA

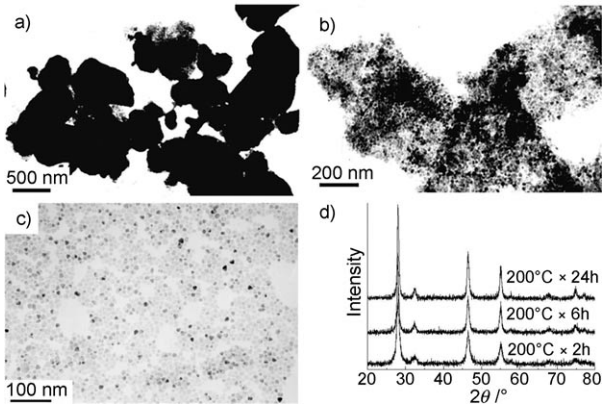

Figure 4. TEM images of $CuInS_2$ synthesized at 200 °C for; a) 2 h, b) 6 h, and c) 24 h, respectively; d) XRD patterns of the products synthesized at 200 °C for different reaction times.

in our system that prevents the surfaces of the newly-born nuclei, or the colloids at the initial stage, from being completely capped. This methodology results in the rapid formation of $CuInS_2$, which was complete within 2 h. The conglomerations of the newly-formed nuclei could not be avoided, owing to their high surface energy. However, in addition to the reaction time, more HDA molecules would further cap the surfaces of colloids during the crystal growth process and provide more steric hindrance. This would result in the conversion of the conglomerations to gradual disperse colloids, as a result of the hydrophobic surface provided by HDAs hydrophobic chains extending into the solvent. Finally, highly monodisperse colloids were obtained if the reaction time was long enough for the colloids to be completely capped by hexadecylamine. Meanwhile, the crystal phase of $CuInS_2$ was unchanged throughout the reaction from 2 h to 24 h. But in the case of $AgInS_2$, the metastable orthorhombic phase existed in a rather narrow range.

To further track the formation of the *o*-$AgInS_2$ metastable phase and the corresponding morphology evolution, along with the reaction time, control experiments were conducted. The products prepared at different reaction times were analyzed by XRD (Figure 5). A mixture of *o*-$AgInS_2$ and Ag_2S

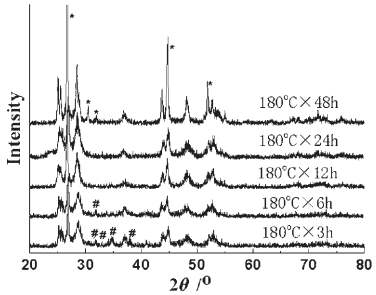

Figure 5. XRD patterns of products for $AgInS_2$ synthesized at 180°C for different reaction time; the crystal phase of Ag_2S (#) and the crystal phase of chalcopyrite-like $AgInS_2$ (*).

was obtained when the reaction time was <6 h at 180°C, and pure *o*-$AgInS_2$ was formed when the reaction time was prolonged to 12–24 h. However, reaction times of up to 48 h produced the low-temperature stable phase of $AgInS_2$ (*c*-$AgInS_2$) in addition to *o*-$AgInS_2$. From the evolution of the crystal phase, we assumed that the co-growth of Ag_2S with $AgInS_2$ at the first reaction stage was a result of the far lower solubility of Ag_2S. However, it was found that freshly formed Ag_2S (because of its higher reactive activity) could still gradually combine with the $In(S_2CNHR)_3$ species or InS_2^- ions in the reaction solution to form *o*-$AgInS_2$ nanocrystals under higher temperature and pressure solvothermal conditions during the crystal growth process. The way that InS_2^- is employed under these conditions is very similar to the way in which $MInS_2$ (M = metal ions) is formed in excess Na_2S in the solvothermal synthesis of $CuInSe_2$ in the presence of $(InSe_2)^-$.[16] If a reaction time of longer than 24 h was used the metastable phase of *o*-$AgInS_2$ would be gradually converted into the low-temperature stable-phase (*c*-$AgInS_2$). The morphological evolution of *o*-$AgInS_2$ colloids is similar to that of $CuInS_2$ colloids, conglomeration, gradual dispersion followed by monodispersion (Figure 6).

Influences of other reaction parameters on the crystal phase and morphologies of $CuInS_2$ and *o*-$AgInS_2$ colloids: Further experiments showed that tetragonal $CuInS_2$ could be prepared in a wider temperature range (120–200°C), while orthorhombic $AgInS_2$ could only be obtained above 160°C (See the Supporting Information, Figure S1). If the reaction temperature was lower than 160°C, no pure *o*-$AgInS_2$ could be obtained. The TEM images of $CuInS_2$ and *o*-$AgInS_2$ colloids synthesized at different reaction temperatures (Figure 7) illustrate that monodisperse colloids can only be obtained if the reaction temperature is beyond the boiling point of the solvent, anisole ($\approx$155.5°C). Substituting HDA with short-chain alkyl amines (e.g., dodecylamine) allowed

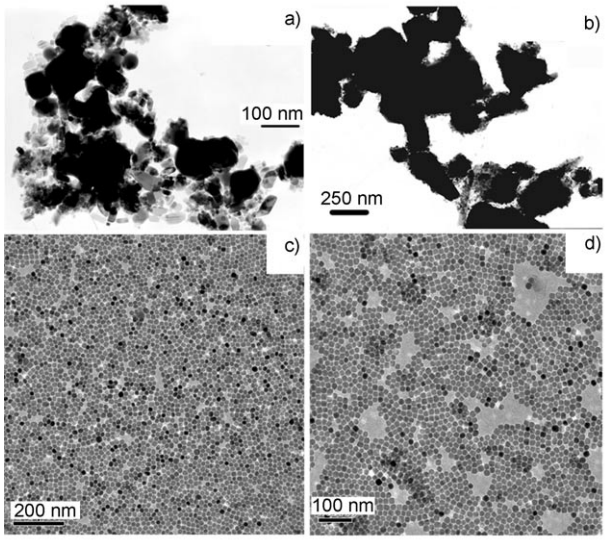

Figure 6. TEM images of products of $AgInS_2$ synthesized at 180°C for different reaction times; a) 3 h, b) 6 h, c) 12 h, and d) 24 h.

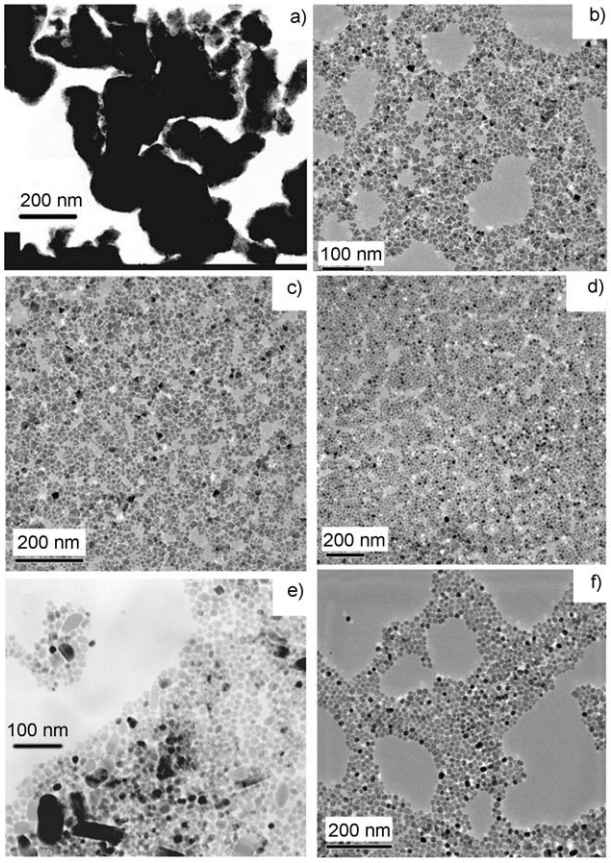

Figure 7. TEM images of $CuInS_2$ synthesized at different reaction temperatures for 12 hours; a) 120°C, b) 160°C, c) 180°C, and d) 200°C. TEM images of products for $AgInS_2$ synthesized at e) 140°C, and f) 160°C.

for the formation of some aggregated nanoparticles. Monodisperse colloids similar to those with HDA as the capping reagent could also be obtained in the presence of longer

chain amines such as octadecylamine (See the Supporting Information Figure S2). These observations were attributed to the different capping abilities of different surfactants. However, in the case of $AgInS_2$ colloids, the products made with dodecylamine as the capping reagent contained small amounts of Ag_2S (See the Supporting Information Figure S3).

Optical properties of $CuInS_2$ colloids: Analysis of the room-temperature UV-vis absorption spectrum (Figure 8a) of the

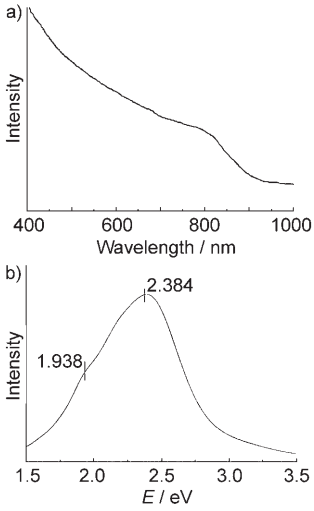

Figure 8. a) UV-vis absorption spectrum measured at room temperature, and b) low-temperature PL spectrum of as-synthesized $CuInS_2$ colloids.

$CuInS_2$ colloids revealed that the colloids absorb in the visible wavelength range, indicating a potential application as a solar absorber. The band gap (Eg) in bulk $CuInS_2$ has been reported as 1.45 eV, corresponding to the UV-vis band around $\lambda = 855$ nm.[2] The lower UV-vis absorptive position of $CuInS_2$ colloids at around $\lambda = 835$ nm in this study showed a blue-shift, this indicates that the size of the $CuInS_2$ colloids is confined. More evidence for the size confinement effect is provided by photoluminescence (PL) spectroscopy (Figure 8b) (recorded at 83 K by using a JY HR 800 UV instrument). The PL spectrum (excited at $\lambda = 325$ nm) of the $CuInS_2$ colloids consisted of two PL subbands concentrated at 1.938 (D1) and 2.384 eV (D2). Both of these bands have a blue-shift, compared with those in bulk $CuInS_2$ materials, this reveals further the size-dependent optical properties of these colloids.[17a] On the other hand, it has been shown that the PL properties of semiconductors are also consistent with their defect structures. Two kinds of defect exist in the defect structure of $CuInS_2$; the donor defect Cu_i, and the acceptor defect V_{In}. Furthermore, there are two types of interstitial position in the chalcopyrite lattice (i1 and i2). Taking the unit cell corners to be defined by the cations (i.e., at each corner Cu or In), these interstitial positions have the coordinates (1/2,1/2,1/4) and (3/4,3/4,3/8), respectively. The first one (i1) is surrounded by six cation sites and four anion sites, and the second one (i2) by four cation sites and six anion sites.[18] Thus, these different interstitial positions result in the varieties of distance among the donor and acceptor defects. Meanwhile, the emission energy from a donor–acceptor pair, separated by a distance r, can be obtained from Equation (3):

$$E_{(r)} = E_g - (E_A^o + E_D^o) + \frac{Z_D Z_A e^2}{\varepsilon r} - \Gamma_{(r)} \quad (3)$$

Here E_g is the band gap energy, the acceptor and donor ionization energies are E_A^o and E_D^o, ε is the dielectric constant, the charges of the donor and acceptor are Z_D and Z_A, respectively, and $\Gamma_{(r)}$ is an additional term, which includes interactions relevant only at very short distances.[17b] Therefore, the D1 and D2 subbands in the PL spectrum of $CuInS_2$ colloids are a result of the recombination of the closest and the second closest donor–acceptor pairs (DAP). This is owed to the donor atom of the DAP occupying an interstitial position within the chalcopyrite lattice and the acceptor atom residing at a cation site next to it. Similar results are also reported by J. Krustok et al.[17]

Conclusion

In summary, monodisperse and single-crystalline pyramidal $CuInS_2$ and rectangular *o*-$AgInS_2$ colloids were successfully synthesized through a facile solvothermal route with hexadecylamine as the capping reagent. A possible mechanism responsible for the crystal growth has been suggested. Control experiments indicated that the morphology and/or phase change of $CuInS_2$ and *o*-$AgInS_2$ colloids was temperature- and/or time-dependent. The optical properties revealed that the as-prepared $CuInS_2$ colloids had an absorption in the visible wavelength range, indicating its potential application as a solar absorber. Furthermore in the present synthesis strategy, the use of alkyl amines or other alkyl acids as capping reagents in the solvothermal process to control the size and morphology of products, to provide a new way for the synthesis of other important pure or doping functional materials, is simple and inexpensive. Our future work will explore the corresponding applications of the obtained colloids in the field of solar cells, linear or nonlinear optical instruments, and light emitting diodes.

Experimental Section

Synthesis of $CuInS_2$ and $AgInS_2$ Colloids: In a typical experiment, $Cu(Ac)_2{\cdot}H_2O$ (0.079 g, 0.4 mmol, analytical reagent (AR)), $InCl_3{\cdot}4H_2O$ (0.117 g, 0.4 mmol, AR) and hexadecylamine (HDA) (1.158 g, 4.8 mmol, 90% mass fraction, Acros) were added to anisole (39 mL, chemically pure) at room temperature. Then the resulting mixture was heated to 60–70 °C and maintained for 1 h with vigorous magnetic stirring. After that, the mixed solution was transferred into a Teflon-lined stainless steel autoclave with a capacity of 50 mL and then carbon disulfide (0.5 mL) was added with magnetic stirring. After the autoclave was sealed, it was

maintained at 200 °C for 12 h in a preheated oven, after which it was removed and allowed to cool to ≈60 °C, and then precipitated by adding methanol into the colloidal solution. Final products were obtained, followed by repeated washing with absolute ethanol, and then drying in vacuum oven at 60 °C. The as-prepared nanocrystals could be re-dispersed in organic solvents, such as toluene, and chloroform.

The synthetic process of *o*-$AgInS_2$ colloids was similar to that of $CuInS_2$ and the typical experiment: $AgNO_3$ (0.068 g, 0.4 mmol), $InCl_3 \cdot 4H_2O$ (0.117 g, 0.4 mmol), hexadecylamine (0.868 g, 3.6 mmol) and CS_2 (0.5 mL), in anisole (39 mL) was treated at 180 °C for 24 h.

Characterization: The phases of the as-prepared products were characterized by using a Rigaku D/Max-2200PC diffractometer equipped with a rotating anode and a $Cu_{k\alpha}$ radiation source ($\lambda = 0.15418$ nm), 2θ ranging from 20° to 80° at a scanning rate of 6°/min. The morphology, crystal lattice and chemical composition of the obtained samples were characterized by transmission electron microscopy (JEOL JEM-100CXII with an accelerating voltage of 100 kV, and JEOL JEM-2010 with an accelerating voltage of 200 kV), high-resolution transmission electron microscopy (JEOL JEM-2100F, with an accelerating voltage of 200 kV), and energy-dispersive X-ray analysis spectroscopy (JEOL JSM- 6460 with an accelerating voltage of 5 kV). The UV-vis absorption spectrum was obtained by using a Perkin–Elmer Lambda 20 UV-vis spectrometer. The photoluminescence (PL) spectra were measured by using a JY HR 800 Uv. A He-Cd laser at a wavelength of 325 nm was used as the excitation source for steady-state PL measurements at 83 K.

Acknowledgements

The work was supported by the National Science Foundation of China (no: 20671061) and the Program for New Century Excellent Talents of Education Ministry of China.

[1] a) J. J. Loferski, *J. Appl. Phys.* **1956**, *27*, 777; b) S. Wagner, P. M. Bridenbugh, *J. Cryst. Growth* **1977**, *39*, 151; c) L. I. Kazmerski, *Inst. Phys. Conf. Ser.* **1977**, *35*, 217; d) S. Cattarin, C. Pagura, L. Armelao, R. Bertoncello, N. Dietz, *J. Electrochem. Soc.* **1995**, *142*, 2818; e) R. S. Roth, H. S. Parker, W. S. Brower, *Mater. Res. Bull.* **1973**, *8*, 333.

[2] a) H. W. Schock in *Solarzellen - Physikalische Grundlagen und Anwendungen in der Photovoltaik* (Eds: D. Meissner), Vieweg & Sohn, Wiesbaden, **1993**, p. 44; b) N. Guezmir, J. Ouerfelli, S. Belgacem, *Mater. Chem. Phys.* **2006**, *96*, 116; c) C. Czekelius, M. Hilgendorff, L. Spanhel, I. Bedja, M. Lerch, G. Müller, U. Bloeck, D. S. Su, M. Giersig, *Adv. Mater.* **1999**, *11*, 643; d) E. Arici, N. S. Sariciftci, D. Meissner, *Adv. Funct. Mater.* **2003**, *13*, 165; e) W. Wettling, *Phys. Blätter* **1997**, *53*, 1197.

[3] a) C. Persson, A. Zunger, *Phys. Rev. Lett.* **2003**, *91*, 266401; b) M. J. Hetzer, Y. M. Strzhemechny, M. Gao, M. A. Contreras, A. Zunger, L. J. Brillson, *Appl. Phys. Lett.* **2005**, *86*, 162105; c) Y. Yan, R. Noufi, K. M. Jones, K. Ramanathan, M. M. Al-Jassim, B. J. Stanbery, *Appl. Phys. Lett.* **2005**, *87*, 121904.

[4] a) Z. Aissaa, T. Ben Nasrallaha, M. Amlouka, J. C. Berne ′deb, S. Belgacema, *Sol. Energy Mater. Sol. Cells* **2006**, *90*, 1136; b) I. V. Bodnar, L. V. Yasyukevich, *J. Mater. Sci.* **1998**, *33*, 183; c) J. Krustok, J. Raudoja, J R. Jaaniso, *Appl. Phys. Lett.* **2006**, *89*, 051905.

[5] a) J. Q. Hu, Q. Y. Lu, K. B. Tang, Y. T. Qian, G. E. Zhou, X. M. Liu, *Chem. Commun.* **1999**, 1093; b) Y. Jiang, Y. Wu, X. Mo, W. C. Yu, Y. Xie, Y. T. Qian, *Inorg. Chem.* **2000**, *39*, 2964; c) D. P. Dutta, G. Sharma, *Mater. Lett.* **2006**, *60*, 2395; d) Q. Y. Lu, J. Q. Hu, K. B. Tang, Y. T. Qian, G. E. Zhou, X. M. Liu, *Inorg. Chem.* **2000**, *39*, 1606; e) K. Wakita, M. Iwai, Y. Miyoshi, H. Fujibuchi, A. Ashida, *Compos. Sci. Technol.* **2005**, *65*,765.

[6] a) L. Tian, H. I. Elim, W. Ji, J. J. Vittal, *Chem. Commun.* **2006**, 4276; b) S. L. Castro, S. G. Bailey, R. P. Raffaelle, K. K. Banger, A. F. Hepp, *Chem. Mater.* **2003**, *15*, 3142; c) K. K. Banger, M. H. C. Jin, J. D. Harris, P. E. Fanwick, A. F. Hepp, *Inorg. Chem.* **2003**, *42*, 7713; d) S. L. Castro, S. G. Bailey, R. P. Raffaelle, K. K. Banger, A. F. Hepp, *J. Phys. Chem. B* **2004**, *108*, 12429; e) T. C. Deivaraj, J. H. Park, M. Afzaal, P. O'Brien, J. J. Vittal, *Chem. Commun.* **2001**, 2304.

[7] a) R. Hunger, R. Scheer, K. Diesner, D. Su, H. J. Lewerenz, *Appl. Phys. Lett.* **1996**, *69*, 3010; b) M. Lin, K. P. Loh, T. C. Deivaraj, J. J. Vittal, *Chem. Commun.* **2002**, 1400; c) M. Ortega-L′opeza, A. Morales-Acevedo, O. Solorza-Feria, *Thin Solid Films* **2001**, *385*, 120.

[8] a) X. L. Gou, F. Y. Cheng, Y. H. Shi, L. Zhang, S. J. Peng, J. Chen, P. W. Shen, *J. Am. Chem. Soc.* **2006**, *128*, 7222; b) M. T. Ng, C. B. Boothroyd, J. J. Vittal, *J. Am. Chem. Soc.* **2006**, *128*, 7118; c) H. L. Peng, D. T. Schoen, S. Meister, X. F. Zhang, Y. Cui, *J. Am. Chem. Soc.* **2007**, *129*, 34.

[9] a) C. B. Burda, X. B. Chen, R. Narayanan, M. A. EI-Sayed, *Chem. Rev.* **2005**, *105*, 1025; b) A. P. Alivisatos, *Science* **1996**, *271*, 933; c) S. Sun, C. B. Murray, D. Weller, L. Folks, A. Moser, *Science* **2000**, *287*, 1989.

[10] a) Y. D. Yin, A. P. Alivisatos, *Nature* **2005**, *437*, 664; b) E. V. Shevchenko, D. V. Talapin, C. B. Murray, S. O'Brien, *J. Am. Chem. Soc.* **2006**, *128*, 3620; c) S. H. Choi, E. G. Kim, T. Hyeon, *J. Am. Chem. Soc.* **2005**, *127*, 3260; d) J. Joo, H. B. Na, T. Yu, J. H. Yu, Y. W. Kim, F. Wu, J. Z. Zhang, T. Hyeon, *J. Am. Chem. Soc.* **2003**, *125*, 11100; e) Y. W. Jun, J. H. Lee, J. S. Choi, J. W. Cheon, *J. Phys. Chem. B* **2005**, *109*, 14795; f) W. W. Yu, X. G. Peng, *Angew. Chem.* **2002**, *114*, 2474; *Angew. Chem. Int. Ed.* **2002**, *41*, 2368.

[11] a) Y. Zhao, Y. Zhang, H. Zhu, G. C. Hadjipanayis, J. Q. Xiao, *J. Am. Chem. Soc.* **2004**, *126*, 6874; b) Y. Li, X. Li, C. Yang, Y. Li, *J. Phys. Chem. B* **2004**, *108*, 16002; c) V. F. Puntes, K. M. Krishnan, A. P. Alivisatos, *Science* **2001**, *291*, 2115.

[12] S. M. Lee, S. N. Cho, J. W. Cheon, *Adv. Mater.* **2003**, *15*, 441.

[13] a) G. Wulff, F. Zeitschrift, *Beitr. Krystallogr. Mineral.* **1901**, *34*, 449; b) J. D. H. Donnay, D. Harker, *Am. Mineral.* **1937**, *22*, 446; c) K. Govender, D. S. Boyle, P. B. Kenway, P. O'Brien, *J. Mater. Chem.* **2004**, *14*, 2575; d) L. H. van Poppl, T. L. Groy, M. T. Caudle, *Inorg. Chem.* **2004**, *43*, 3180.

[14] a) B. Liu, H. C. Zeng, *J. Am. Chem. Soc.* **2003**, *125*, 4430; b) W. S. Seo, J. H. Shim, S. J. Oh, E. K. Lee, N. H. Hur, J. T. Park, *J. Am. Chem. Soc.* **2005**, *127*, 6188; c) J. Joo, G. K. Soon, J. H. Yu, T. Hyeon, *Adv. Mater.* **2005**, *17*, 1873; d) Y. W. Jun, M. F. Casula, J. H. Sim, S. Y. Kim, J. Cheon, A. P. Alivisatos, *J. Am. Chem. Soc.* **2003**, *125*, 15981.

[15] a) X. Wang, J. Zhuang, Q. Peng, Y. D. Li, *Nature* **2005**, *437*, 121; b) A. B. Panda, G. Glaspell, M. S. EI-Shall, *J. Am. Chem. Soc.* **2006**, *128*, 2790; c) M. B. Sigman, A. Ghezelbash, T. Hanrath, A. E. Saunders, F. Lee, B. A. Korgel, *J. Am. Chem. Soc.* **2003**, *125*, 16050.

[16] a) X. M. Gu, in *The series of Inorganic Chemistry, Vol. 2: Be, Alkaline earth and Al, Ga Secondly Groups.* (Eds: Y. S. Gong, X. W. Zang, K. L. Tang, Y. Y. Lu, W. Z. Zeng), Scientific Publishing Company, Beijing, **1990**, p. 608; b) B. Li, Y. Xie, J. X. Huang, Y. T. Qian, *Adv. Mater.* **1999**, *11*, 1456.

[17] a) J. Krustok, J. H. SchÖn, H. Collan, M. Yakushev, J. Mädasson, E. Bucher, *J. Appl. Phys.* **1999**, *86*, 364; b) J. Krustok, J. Raudoja, J. H. SchÖn, M. Yakushev, H. Collan, *Thin Solid Films* **2000**, *361–362*, 406.

[18] G. Brandt, A. Raeuber, J. Schneider, *Solid State Commun.* **1973**, *12*, 481.

Received: April 24, 2007
Published online: July 26, 2007

